

# Overexpression of PKM $\zeta$ Alters Morphology and Function of Dendritic Spines in Cultured Cortical Neurons

Shiri Ron, Yadin Dudai and Menahem Segal

Department of Neurobiology, The Weizmann Institute of Science, Rehovot 76100, Israel

Address correspondence to email: menahem.segal@weizmann.ac.il.

**Protein kinase M zeta (PKM $\zeta$ ), an atypical isoform of protein kinase C (PKC), has been implicated in long-term maintenance of neuronal plasticity and memory. However, the cellular machinery involved in these functions has yet to be elucidated. Here, we investigated the effects of PKM $\zeta$  overexpression on the morphology and function of cortical neurons in primary cultures. Transfection with a plasmid construct expressing the PKM $\zeta$  gene modified the distribution of spine morphologies and reduced spine length, while leaving total spine density and dendritic branching unchanged. A significant increase in magnitude but not frequency of miniature excitatory post synaptic currents was detected in the PKM $\zeta$  overexpressing cells. These results suggest that PKM $\zeta$  is involved in regulation of dendritic spine structure and function, which may underlie its role in long-term synaptic and behavioral plasticity.**

**Keywords:** confocal imaging, dendritic spines, long-term plasticity, memory storage, structural plasticity

## Introduction

Ample evidence indicates that the atypical protein kinase C (PKC) isoform, protein kinase M zeta (PKM $\zeta$ ), plays a key role in the maintenance phase of long-term potentiation (Sacktor et al. 1993; Osten et al. 1996; Ling et al. 2002; Serrano et al. 2005; Kelly et al. 2007) and in long-term memory storage (Pastalkova et al. 2006; Shema et al. 2007, 2009, 2011; Serrano et al. 2008; Kwapis et al. 2009; Hardt et al. 2010; von Kraus et al. 2010). The mechanism in which PKM $\zeta$  exerts these functions, however, is not yet fully understood. Recently, it has been proposed that PKM $\zeta$  upregulates the trafficking of GluR2-containing AMPA receptors into postsynaptic sites, thus augmenting synaptic efficacy (Ling et al. 2006; Yao et al. 2008; Miguez et al. 2010; Sacktor 2011). Morphological alterations in synaptic structures have been implicated in lasting alterations of synaptic efficacy and memory (Bailey and Kandel 1993; Yuste and Bonhoeffer 2001; Lamprecht and LeDoux 2004; Segal 2005; Bourne and Harris 2008; De Roo et al. 2008; Yang et al. 2009; Kasai et al. 2010). In particular, short large spines are considered to be stable “memory” spines, whereas thin long protrusions are the more plastic ones (Kasai et al. 2010). Thus, investigating the role of PKM $\zeta$  in morphological plasticity may shed light on its function in the synapse and its contribution to long-term cellular and behavioral plasticity.

Here, we report the effects of PKM $\zeta$  overexpression on selected attributes of morphology and function of rat cortical neurons grown in dissociated cultures. Toward this end, primary cortical neurons were transfected with the PKM $\zeta$  gene or a dominant negative mutated form of the enzyme (DN) under the control of a cytomegalovirus (CMV) promoter. Using

confocal microscopy, dendritic branching and spine size, shape, and density were examined. Furthermore, electrophysiological recordings were used in an attempt to unveil modification in synaptic function associated with PKM $\zeta$  overexpression. Our data indicate that PKM $\zeta$  regulates dendritic spine structure and synaptic function.

## Materials and Methods

### Cultures

Cultures were prepared as previously detailed (Goldin et al. 2001). Rat pups were decapitated at postnatal day 3, and their brains were removed and placed in a chilled (4 °C), oxygenated Leibovitz L15 medium (Gibco) enriched with 0.6% glucose and Gentamicin (Sigma; 20  $\mu$ g/mL). Bilateral cortices were dissected out and collected in the same medium. Cortical tissue was mechanically dissociated with a sterile pipette tip after incubation with trypsin (0.25%) and DNAase (50  $\mu$ g/mL) in Hank's buffered salt solution (Sigma) and passed to the plating medium consisting of 5% heat-inactivated horse serum (HS), 5% fetal calf serum, B-27 (1  $\mu$ L/1 mL), and 4-(2-hydroxyethyl)-1-piperazineethanesulfonic acid (HEPES, 25 mM) prepared in minimum essential medium (MEM)-Earl salts (Gibco), enriched with 0.6% glucose, Gentamicin (20  $\mu$ g/mL), and 2 mM GlutaMax (Gibco) (enriched MEM). Approximately  $4 \times 10^5$  cells in 1 mL of medium were plated in each well of a 24-well plate or on 35 mm glass bottom petri dishes, onto a cortical glial feeder layer which was grown on the glass for 2 weeks before the plating of the neurons. Cells were left to grow in the incubator at 37 °C, 5% CO<sub>2</sub> for 4 days, at which time the medium was changed to 10% HS in enriched MEM, plus a mixture of 5'-fluoro-2'-deoxyuridine/uridine (Sigma; 20  $\mu$ g and 50  $\mu$ g/mL, respectively), to block glial proliferation. The medium was replaced 5 days later by 10% HS in MEM and no further changes were made until cultures were used for experimentation.

### Transfections

Transfections were conducted on cells at 7–8 days in vitro (DIV), before changing the medium to 10% HS. A Lipofectamine 2000 (Invitrogen) mix was prepared at 1–1.2  $\mu$ L/well with 50  $\mu$ L/well OptiMEM (Invitrogen) and incubated for 5 min at room temperature. This was mixed with 1–1.3  $\mu$ g/well total DNA in 50  $\mu$ L/well OptiMEM and incubated for 20 min at room temperature. The mix was then added to the culture wells and allowed to incubate for 2–4 h before changing the medium. In all cases, at least several neurons were transfected in each well. In these experiments, 3 constructs were used: 1) PKM $\zeta$  subcloned into the lentiviral expression vector, pCSC-IRES/GFP (IRES, internal ribosomal entry site, GFP, green fluorescent protein) (pCSC-SP-PW-PKM $\zeta$ -IRES-GFP, “PKM $\zeta$ <sub>OE</sub>”); 2) A dominant negative mutated form of PKM $\zeta$ , with a point mutation in amino acid 128 (K281W), cloned into pCSC-IRES/GFP (pCSC-SP-PW-DN-IRES-GFP, “DN”); 3) For control, a construct containing only GFP under the same promoter and internal ribosomal entry site (pCSC-SP-PW-IRES-GFP, “Control”).

All vectors consisted of a CMV promoter and contained the enhanced GFP coding sequence following an IRES sequence, allowing identification and morphological examination of the transfected neurons. The reporter GFP and the PKM $\zeta$ /DN products are translated separately from

the same mRNA due to the separating IRES sequence and are suggested to be translated at a rate of 1–10, respectively.

For synapse confirmation, a PSD-95/DsRed construct was cotransfected with the constructs mentioned above. For construct purification, Wizard Plus Midipreps DNA purification kit (Promega) was used.

### Live Imaging

For live imaging, cover glasses bearing transfected cortical cultures were placed in a specially made perfusion chamber preheated to 36 °C and containing standard extracellular solution (NaCl 129 mM, KCl 4 mM, MgCl<sub>2</sub> 1 mM, CaCl<sub>2</sub> 2 mM, glucose 10.5 mM, and HEPES 10 mM). The chamber was then placed on the stage of a Zeiss LSM 510 laser scanning confocal microscope. Transfected cells were imaged with a 40× oil-immersion objective lens (1.3 numerical aperture [NA]). Detector gain and amplifier were initially set to obtain pixel densities within a linear range. Confocal image z-stacks of transfected neurons were recorded using 0.7× scan zoom for whole cell analysis. For spine analysis, image stacks of dendritic segments were captured with 1–3× scan zoom. When needed, the 2-channel option of the confocal microscope was used to take simultaneous images with excitation wavelengths of 488 and 543 nm. Extracellular solution was changed every 30 min in order to maintain optimal osmotic concentration and temperature. For long-term time-lapse imaging over several days, coordinates of the detected neurons were logged for future location at the subsequent time points.

### Morphological Analysis

Image analysis was conducted off-line on 3D image stacks using the Zeiss LSM image browser to navigate through the stacks.

### Sholl Analysis

Image stacks (0.7×) of transfected pyramidal neurons were used for sholl analysis. Concentric circles centered at the cell body were drawn with increasing radii of 20 μm (20–120 μm range). Dendritic arbor properties were manually examined by calculating the number of dendrites intersecting with each radius. ImagePro+ software was used for counting of the marked intersections.

### Spine Analysis

An average of 2 separate dendritic segments (30–80 μm each) per neuron was randomly chosen from secondary or tertiary branches for spine analysis. For spine length analysis, all protrusions were measured from their dendritic base to the tip (including spine head). Protrusions were then manually categorized into spines longer than 2 μm (“long”), spines shorter than 2 μm (“short”), “stubby” spines (no spine neck), “mushroom” spines (0.5 μm neck or shorter and with wide mushroom shaped heads), and filopodia (long, headless protrusions). Average segment length and type (secondary/tertiary) was similar between groups. The averaged distance of dendritic segment from soma was similar between groups and exceeded 40 μm from the soma. Results were calculated by average per neuron. A total of 18 neurons were examined in the *PKMζ<sub>OE</sub>* group (total dendritic length: 1956 microns, total number of spines: 1065), 22 neurons in the *Control* group (total dendritic length: 2326 microns, total number of spines: 1470), and 8 neurons in the *DN* group (total dendritic length: 738 microns, total number of spines: 348).

### Immunocytochemistry

For immunostaining, cover glasses bearing transfected primary cortical cells were washed briefly with standard balanced salt solution (NaCl 129 mM, KCl 4 mM, MgCl<sub>2</sub> 1 mM, CaCl<sub>2</sub> 2 mM, glucose 10.5 mM, and HEPES 10 mM), fixed in 4% paraformaldehyde in 0.1 M PBS, pH 7.4, for 15 min, and washed with phosphate buffered saline (PBS) thoroughly. For fluorescence staining, cultures underwent protein blocking with 10% normal goat serum and 0.1% Triton X-100 in PBS for 1 h. Subsequently, cultures were incubated overnight at 4 °C with rabbit polyclonal anti-PKMζ antibody (Hernandez et al. 2003, a gift from Dr T.C. Sacktor; SUNY Downstate Medical Center, Brooklyn, NY, 1:1000) or rabbit anti-cleaved caspase 3 (Santa Cruz; 1:500). Cultures

were then incubated for 1 h with Alexa Fluor 546-labeled goat anti-rabbit secondary antibody (Invitrogen; 1:200). Coverslips were transferred onto glass slides and mounted for visualization with antifading mounting medium. Confocal image stacks were recorded as mentioned previously (live imaging). Fluorescence intensity of immunostained cultures was measured using the Image-J software package.

### Electrophysiology

Cortical cultures at 14–15 DIV were transferred to a recording chamber placed on the stage of an inverted Olympus IX70 microscope and washed with a standard recording medium, containing (in mM) NaCl, 129; KCl, 4; CaCl<sub>2</sub>, 2; MgCl<sub>2</sub>, 1; Glucose, 10; HEPES, 10; tetrodotoxin 0.5 μM; and bicuculline, 20 μM; pH 7.4, 330 mOsm. Neurons were recorded with whole cell patch pipettes containing (in mM): K-gluconate, 136; KCl, 10; NaCl, 5; HEPES, 10; ethylene glycol-bis (beta-aminoethyl ether) N,N,N',N'-tetra-acetic acid, 0.1; Na-GTP, 0.3; Mg-ATP, 1; and phosphocreatine, 5; pH 7.2 with a resistance in the range of 5–10 MΩ. Transfected neurons were visualized with a Till Photonics fluorescent light source. The cells were held at –60 mV, and their monitored series resistance and capacitance were not changed significantly throughout the recording session. Signals were amplified with MultiClamp 700B, recorded with pClamp9 (Axon Instruments, Foster City, CA) filtered and analyzed using MiniAnalysis and Origin software.

### Data Analysis

Off-line measurements were conducted in a double blind procedure to assure unbiased observations. Statistical comparisons were made using student's *t*-tests (2 tailed) for comparisons of 2 groups and one-way analysis of variance (ANOVA) with a follow up Bonferroni post hoc comparison for 3 groups. Kolmogorov-Smirnov test was used for distribution analyses and Mann-Whitney *U* test was used for non-parametric testing. *P* < 0.05 was considered significant in all cases. Averaged data are shown as mean ± standard error of the mean.

## Results

### Transfection Resulted in Robust Expression of the PKMζ/DN Protein

Overexpression of the PKMζ protein and the DN form was detected in neurons transfected with the *PKMζ<sub>OE</sub>* and *DN* constructs, respectively, while only low levels of endogenous PKMζ were detected in the somata of *Control* and non-transfected neurons (Fig. 1). Since morphological parameters were visualized using the GFP reporter gene, the optimal expression pattern of the reporter gene following transfection was examined. To this end, we time-lapsed images of transfected cultures in glass bottom petri dishes every 24 h for 4 days starting at 24 h after transfection (AT). Transfected cell fluorescence was detected at all 4 time points. Overall, fluorescence intensity was stable between 48 and 96 h AT in most neurons of the 3 transfection groups (*PKMζ<sub>OE</sub>*, *DN*, and *Control*) (Supplementary Fig. S1).

### Transfection Did Not Affect Neuronal Survival

In order to ensure that the robust expression of the PKMζ or DN protein, detected in transfected cells, did not induce neuronal stress and promote cell apoptosis, cultures were stained for the activated apoptotic factor, cleaved caspase 3 (Supplementary Fig. S2A). No significant difference in cleaved caspase 3 staining intensity was detected between nontransfected and transfected neurons in both transfection groups (Supplementary Fig. S2B,C).

Furthermore, using phase-contrast and fluorescence imaging, cell bodies of transfected cells were inspected for vacuolar structures, which may indicate neuronal necrosis (Supplementary

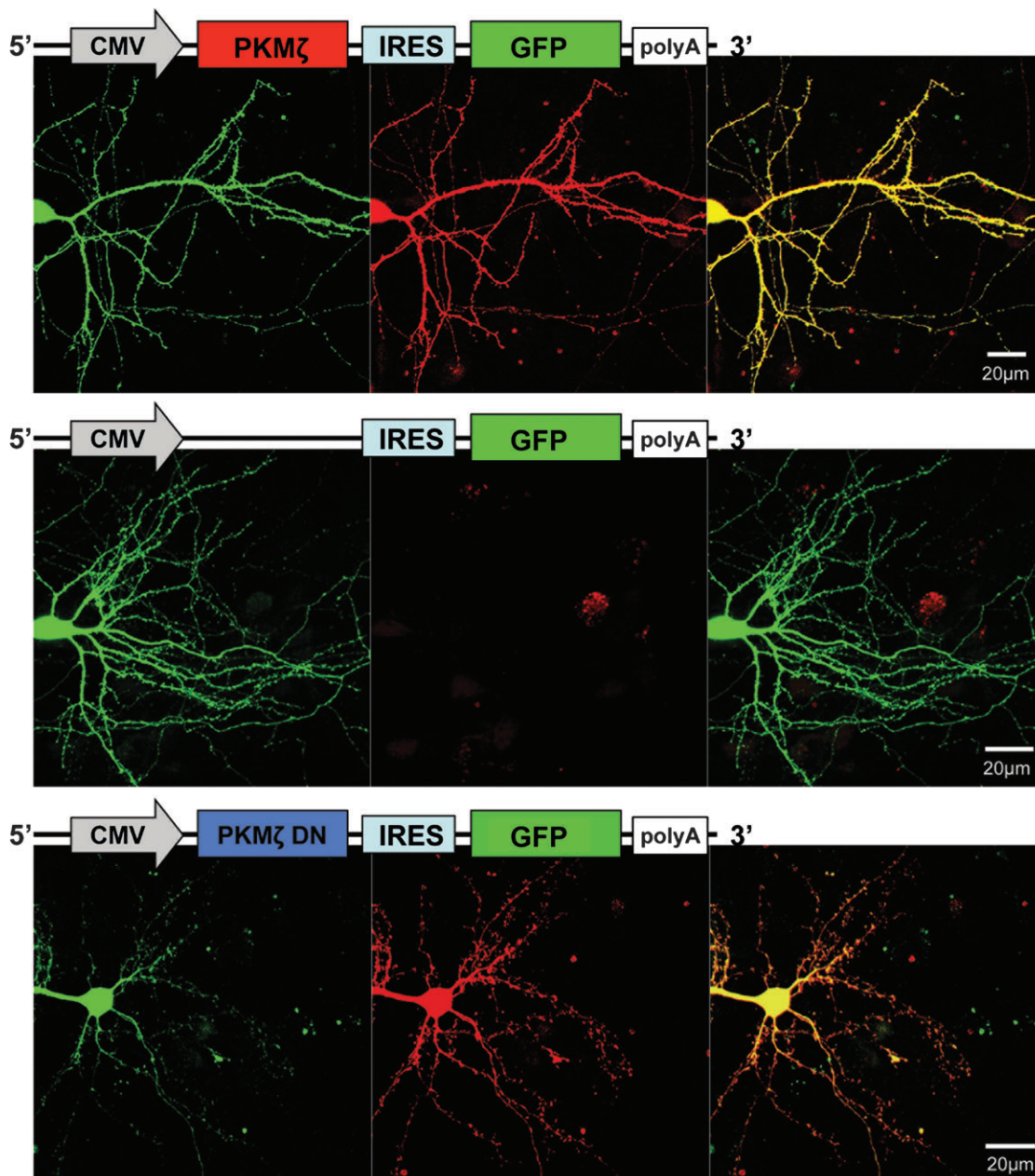


**Figure 1.** Transfection leads to a vast overexpression of PKM $\zeta$  and the dominant negative form of PKM $\zeta$  (DN) in comparison with *control*. Following transfection at 8 DIV, neurons were fixed 24–96 h later and stained for PKM $\zeta$  (Rb polyclonal  $\alpha$ PKM $\zeta$ , 1:1000). Since the PKM $\zeta$  antibody detects a region of the catalytic domain of the enzyme that was not mutated, the DN form is also recognized. PKM $\zeta$  overexpression is detected in neurons transfected with the *PKM $\zeta$ <sub>OE</sub>* (top) and *DN* constructs (bottom), while only low endogenous PKM $\zeta$  levels are detected in neurons transfected with the *Control* construct (center). *Green*—reporter GFP, *Red*—PKM $\zeta$  staining, *Yellow*—merged images. A schematic map of the transfected constructs is shown for each image set.

Fig. S2D–F). Transfected neurons did not show a particular tendency toward cell necrosis.

#### ***PKM $\zeta$ Overexpression Did Not Affect Dendritic Arborization***

The morphology of the dendritic arbor of a neuron is a critical determinant of its function, in that it reflects the number and types of synapses available and how synaptic signals are processed (Parrish et al. 2007). We examined the effects of PKM $\zeta$  overexpression on the dendritic structure of cortical neurons, using Sholl analysis (Sholl 1953). Clear images of pyramidal neurons transfected with *PKM $\zeta$ <sub>OE</sub>* ( $n = 8$  neurons) or

*Control* ( $n = 8$  neurons) were selected (Fig. 2A,B) at 11–12 DIV (i.e., 14–15 days old). No significant difference in dendritic branching was found between PKM $\zeta$  overexpressing neurons and control (Fig. 2C, student's *t*-test).

#### ***PKM $\zeta$ Overexpression Altered Protrusion Length***

The morphological effects of PKM $\zeta$  overexpression on dendritic spines were examined in transfected spiny neurons at 11–12 DIV (72–96 h after transfection). At this age, the culture is nearly mature and synaptic connections among neurons stabilize and spines form such that effects of various treatments can be easily detected. Live confocal imaging was carried out

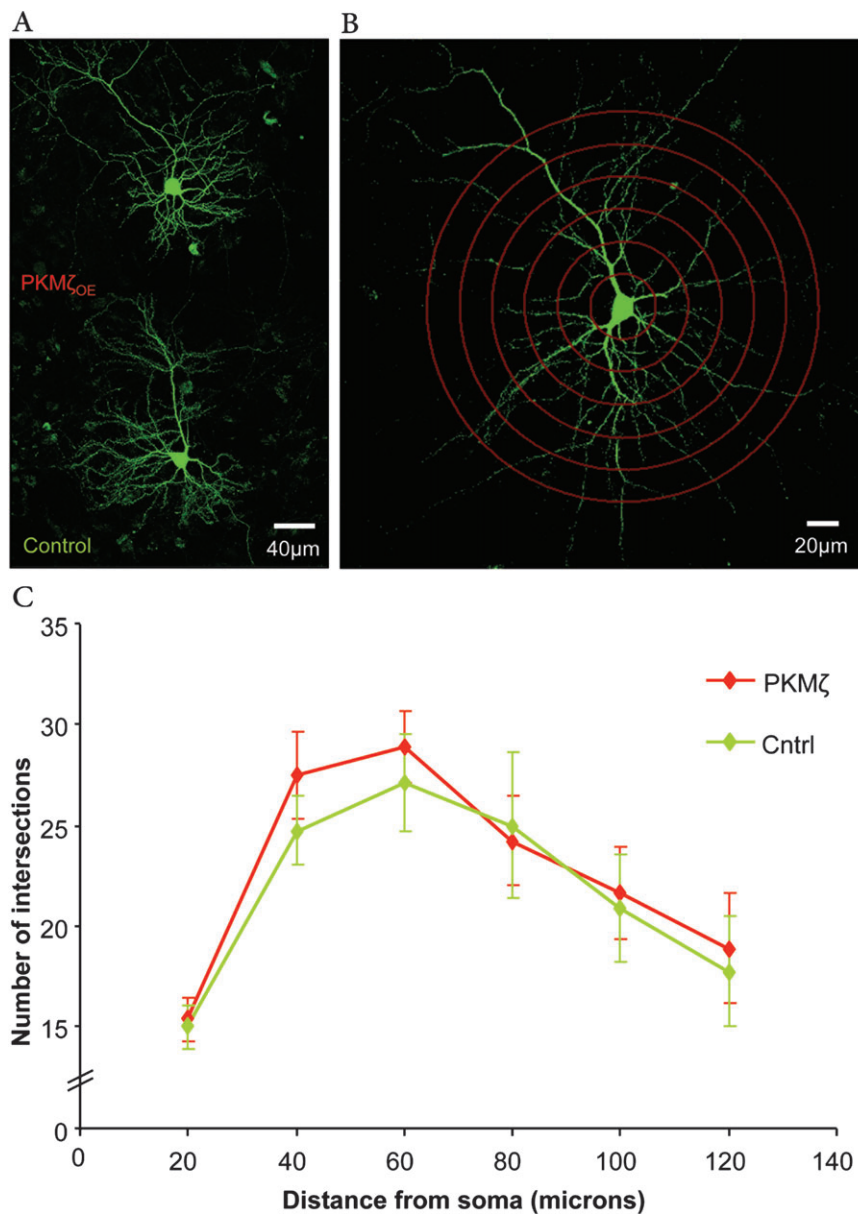


**Figure 2.** PKM $\zeta$  overexpression does not affect dendritic arborization (A) Representative images of 11–12 DIV, pyramidal cortical neurons selected for sholl analysis following transfection with the PKM $\zeta_{OE}$  (top) or *Control* construct (bottom). (B) For the Sholl outline, concentric circles, centered at the soma, were drawn with increasing radii of 20  $\mu$ m. Branching characteristics were determined by counting the number of dendrites intersecting with each radius. (C) No significant difference in dendritic branching is found between PKM $\zeta$  overexpressing and Control neurons.  $n = 8$  neurons per group, results are expressed as mean  $\pm$  standard error of the mean.

on neurons from the 3 transfection groups in 3 (PKM $\zeta_{OE}$ , *Control*) and 4 (*DN*) separate experiments. Images were then taken for blind analysis using Zeiss LSM imaging browser. An average of 2 separate secondary/tertiary dendritic segments (30–80  $\mu$ m each) per neuron was randomly selected for spine analysis (Fig. 3A). The length of all protrusions on a selected segment was measured from the dendritic base of the protrusion to its tip (including the spine head). Protrusions that were not clear and thus could not be measured properly were not included in the analysis and constituted 1–3% of all protrusions. PKM $\zeta$  overexpression led to a significant reduction in average spine length (Fig. 3B, one-way ANOVA,  $F_{2,45} = 17.32$ ,  $P < 0.00001$ ) and resulted in a significantly different distribution of spine lengths (Fig. 3C, Kolmogorov–smirnov test, PKM $\zeta_{OE}$  vs. *Control*— $P = 4.1140 \times 10^{-27}$ , *DN* vs. *Control*—non significant

[ $P = 0.5450$ ]). That said, total protrusion density did not significantly differ between the 3 transfection groups (Fig. 3D).

#### PKM $\zeta$ Overexpression Altered Dendritic Spine Morphology

Spines differ from one another in length as well as shape. The shape of a dendritic spine has been shown to contribute to its synaptic qualities. To determine whether PKM $\zeta$  overexpression altered the distribution of spine shape, protrusions measured for length were categorized into 5 different groups based on shape and size (Fig. 4A). Spines that did not fall under any category were categorized “undefined” and constituted 10–13% of all spines. Neurons overexpressing PKM $\zeta$  displayed a specific repertoire of dendritic spines compared with both the *DN* and *Control* groups which displayed similar spine morphologies. The percentage of long spines ( $\geq 2 \mu$ m) and

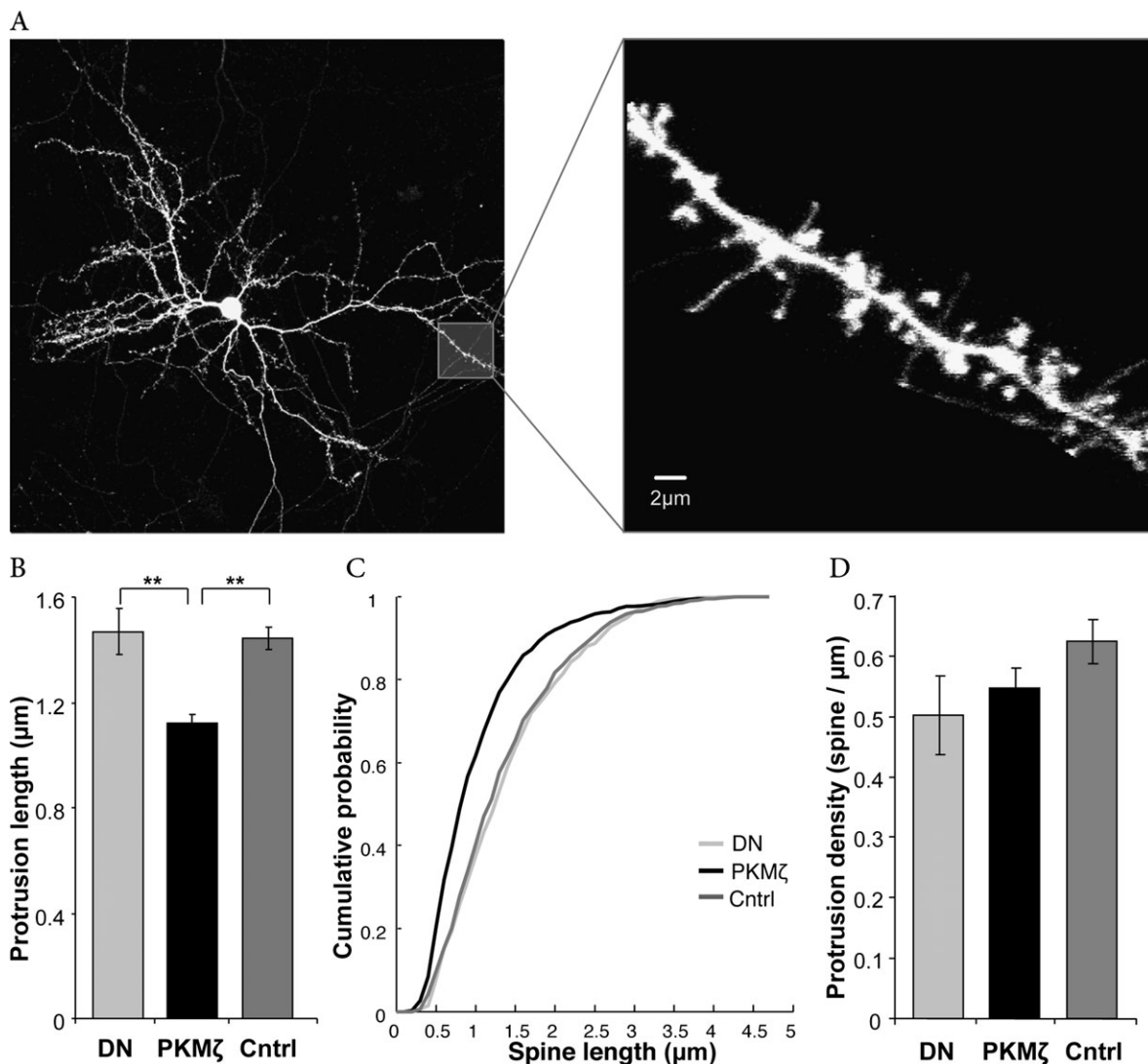


**Figure 3.** PKM $\zeta$  overexpression alters protrusion length. The effects of PKM $\zeta$  overexpression on dendritic protrusion length were examined in live transfected spiny neurons at 11–12 DIV (72–96 h after transfection), imaged with a confocal microscope. (A) An average of 2 separate dendritic segments (30–80  $\mu\text{m}$  each) per neuron was randomly selected for spine analysis. (B) PKM $\zeta$  overexpression leads to a significant decrease in average spine length. (C) PKM $\zeta$  overexpression results in a significantly different distribution of spine lengths depicted by cumulative probability ( $P < 0.0001$ , kolmogorov-smirnov test) (D) Total spine density does not significantly differ between the 3 transfection groups. \* $P < 0.01$ , \*\* $P < 0.001$ , one-way ANOVA followed by Bonferroni post hoc analysis, results are expressed as mean  $\pm$  standard error of the mean.

filopodia was smaller than *Control* (Fig. 4B, long spines—*one-way ANOVA*,  $F_{2,45} = 27.15$ ,  $P < 0.00001$ ; and filopodia— $F_{2,45} = 5.02$ ,  $P = 0.011$ , post hoc comparisons showed no significant difference between PKM $\zeta_{OE}$  and DN, whereas PKM $\zeta_{OE}$  differed from *Control* [ $P < 0.01$ ]). The percentage of stubby spines was significantly higher in the PKM $\zeta_{OE}$  transfection group (Fig. 4C, *one-way ANOVA*,  $F_{2,45} = 24.71$ ,  $P < 0.00001$ ). Furthermore, a trend toward a higher percentage of mushroom spines in PKM $\zeta$  overexpressing neurons, in comparison with the DN group, was identified (Fig. 4C). Overall, PKM $\zeta$  overexpression led to an increase in mature spine density (stubby + mushroom, Irwin et al. 2000; Restivo et al. 2005; Camera et al. 2008) (Fig. 4D, *one-way ANOVA*,  $F_{2,45} = 25.52$ ,  $P < 0.00001$ ). Average segment length for analysis was similar between groups (Supplementary Fig. S3). Results were calculated by average per neuron. A total of 18 neurons were examined in the PKM $\zeta_{OE}$  group (total dendritic length: 1956  $\mu\text{m}$ , total number of spines: 1065) 22 neurons in the *Control* group (total dendritic length: 2326  $\mu\text{m}$ ,

total number of spines: 1470) and 8 neurons in the DN group (total dendritic length: 738  $\mu\text{m}$ , total number of spines: 348).

The difference in spine morphologies between *Control* and PKM $\zeta_{OE}$ -transfected neurons may reflect a difference in rate of maturation of spines, a genuine effect of the peptide on steady state, “memory storage” spines, or both. To examine this, we studied the morphological effects of PKM $\zeta$  on spines of fully matured neurons at 18 DIV ( $n = 10$  neurons in each group, Fig. 5A). The fraction of long spines was significantly larger in the *Control* group (Fig. 5B,  $P < 0.001$ , student’s *t*-test). Furthermore, results showed a significantly higher fraction of stubby and mushroom spines (=“mature” spines) in the PKM $\zeta_{OE}$  group compared with *Control* (Fig. 5C,D). Total protrusion density was similar in the 2 groups (Fig. 5E) and was significantly elevated compared with 11–12 DIV neurons. (PKM $\zeta_{OE}$ —0.55 vs. 1.06 spines/ $\mu\text{m}$ ,  $P < 0.001$  and *Control*—0.62 vs. 0.95 spines/ $\mu\text{m}$ ,  $P < 0.001$ , student’s *t*-test). No significant difference in mature spine density was seen when

A

Protrusion type	Description
Stubby	no neck
Mushroom	neck $\leq 0.5\mu\text{m}$ , head $>0.5\mu\text{m}$
Short	head + neck $<2\mu\text{m}$ in length
Long	head + neck $\geq 2\mu\text{m}$ in length
Filopodia	headless protrusion

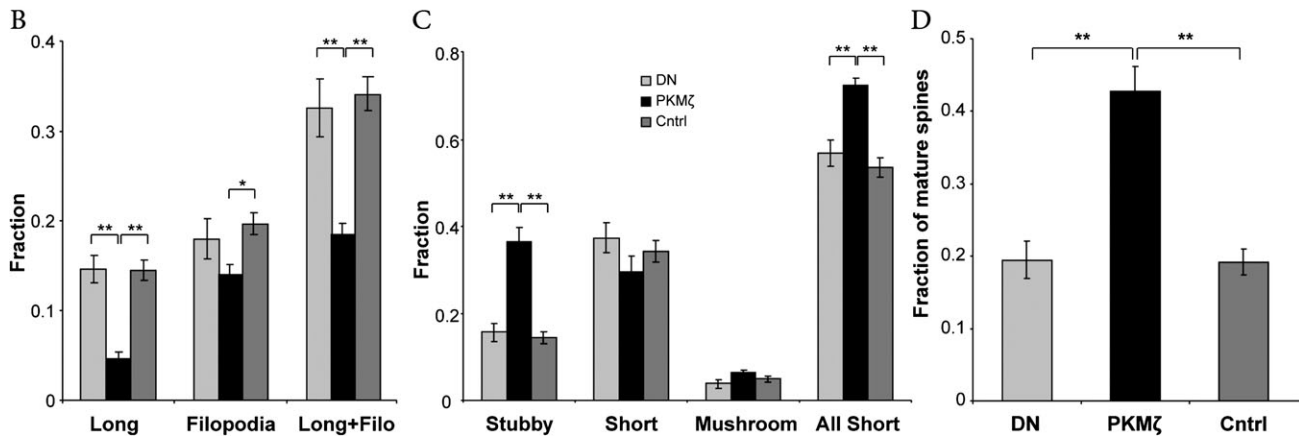
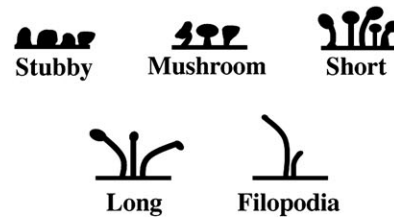


**Figure 4.** PKM $\zeta$  overexpression alters dendritic spine morphology. (A) Protrusions measured for length were categorized into 5 different groups based on shape and size (B) PKM $\zeta$  overexpression results in a decrease in percentage of long spines ( $\geq 2\mu\text{m}$ ) and filopodia. The total fraction of long and filopodia protrusions detected in PKM $\zeta$ OE neurons is significantly reduced in comparison with DN and Control. (C) PKM $\zeta$  overexpression results in the expression of a significantly higher percentage of stubby spines. The percentage of short spines is slightly reduced in neurons overexpressing PKM $\zeta$ . Furthermore, a strong trend toward a higher percentage of mushroom spines is detected in the PKM $\zeta$ OE group compared with DN. Overall, the total fraction of “all short” (spine length  $< 2\mu\text{m}$ ) protrusions detected in PKM $\zeta$ OE neurons is significantly higher than in DN and Control neurons. (D) PKM $\zeta$  overexpression leads to an increase in mature spine (stubby + mushroom) density. Results were calculated by average per neuron and demonstrate mean  $\pm$  standard error of the mean (SEM). PKM $\zeta$ OE— $n = 18$  cells (total dendritic length: 1956  $\mu\text{m}$ , total number of spines: 1065), Control— $n = 22$  cells (total dendritic length: 2326  $\mu\text{m}$ , total number of spines: 1470), DN— $n = 8$  cells (total dendritic length: 738  $\mu\text{m}$ , total number of spines: 348). \* $P < 0.01$ , \*\* $P < 0.001$ , one-way ANOVA followed by Bonferroni post hoc analysis, results are expressed as mean  $\pm$  SEM.

comparing between 11–12 DIV PKM $\zeta$ OE neurons with 18 DIV neurons of the same transfection group. The same comparison in the Control group showed a significantly higher fraction of mature spines in the 18 DIV neurons ( $P < 0.05$ , student's  $t$ -test) (Fig. 5F). All in all, these results indicate that overexpression of PKM $\zeta$  is instrumental in changing spine morphologies also in mature neurons and that PKM $\zeta$  overexpression might be causing both an early maturation of spines but in a significantly higher percentage of protrusions.

We verified that the large number of stubby spines detected in the PKM $\zeta$  overexpressing neurons represent genuine synapses, by cotransfecting the PKM $\zeta$ OE construct with PSD-95. This is a scaffold protein that forms the backbone of postsynaptic protein complexes. With this postsynaptic marker, we could detect spines that represent genuine synapses (Fig. 6A). Imaging of cotransfected neurons identified PSD-95 in more than 85% of all spines and in more than 90% of all stubby spines (Fig. 6B,  $n = 3$  cotransfected neurons, 336 spines). Thus, more than 85% of the dendritic spines identified in PKM $\zeta$  overexpressing neurons, including stubby spines, represent genuine synapses.

#### PKM $\zeta$ Overexpression Did Not Affect Stubby Spine Size

Spine head expansion following local synaptic activation has been reported in several cases (Matsuzaki et al. 2004; Zhou et al. 2004; Segal 2005), and it has been suggested that the insertion of glutamate receptors might be the cause for this expansion (Kopeck et al. 2007; Korkotian and Segal 2007). Since

stubby spines were most prevalent in neurons overexpressing PKM $\zeta$ , head size of these stubby spines was assessed. Head perimeter of stubby spines was measured in 11–12 DIV neurons transfected with the PKM $\zeta$ OE/DN/Control constructs (PKM $\zeta$ OE— $n = 13$  neurons, 122 stubby spines, DN— $n = 6$  neurons, 30 stubby spines, Control—14 neurons, 67 stubby spines). These neurons were randomly selected from the group of neurons taken for protrusion length and shape analysis. No significant difference in head size was detected between groups though a slight trend in head size enlargement was seen in the PKM $\zeta$  overexpression group (Supplementary Fig. S4).

#### Overexpression of PKM $\zeta$ Affected mEPSCs

Recordings were made from 36 PKM $\zeta$ OE transfected, 2-week old neurons and 27 age matched Control neurons in 10 different experiments (Fig. 7A). Standard 2 min recording sessions were made from each cell. The mean mEPSC frequency (/2 min) was not different between the 2 groups (Fig. 7B, being  $37.83 \pm 6.1$  for the PKM $\zeta$ OE group and  $36.96 \pm 7.1$  events for the Control). Likewise, there was no difference in the kinetics of rise and decay average times of the 2 groups ( $3.2 \pm 0.2$  ms and  $3.9 \pm 0.3$ , respectively, for the PKM $\zeta$ OE group and  $2.8 \pm 0.2$  ms and  $3.5 \pm 0.2$  for the Control). There was a slight nonsignificant difference between PKM $\zeta$ OE and Control neurons in the average magnitudes of the mEPSCs ( $14.2 \pm 1.1$  pA and  $11.9 \pm 0.7$  pA, respectively). Further analysis of the mEPSC average amplitude per neuron indicated a non-Gaussian distribution in both the

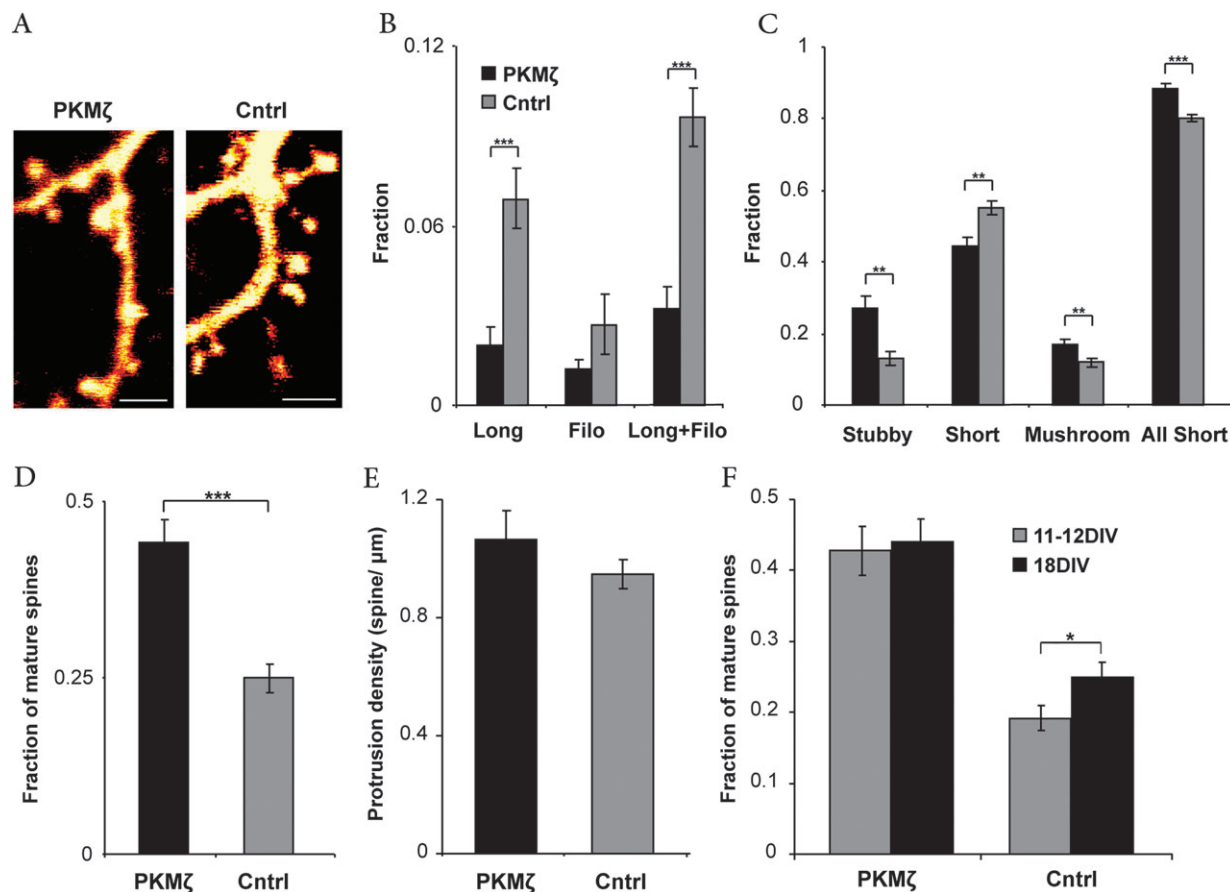


**Figure 5.** PKM $\zeta$  overexpression increases mature spine fraction in fully matured neurons in culture. (A) Neurons transfected at 8 DIV were examined for spine morphology at 18 DIV. (B) PKM $\zeta$  overexpression results in a decrease in percentage of long spines ( $\geq 2 \mu\text{m}$ ). The total fraction of long and filopodia protrusions detected in PKM $\zeta_{OE}$  neurons is significantly reduced in comparison with Control. (C) PKM $\zeta$  overexpression results in the expression of a significantly higher percentage of stubby and mushroom spines. The percentage of short spines is significantly reduced in neurons overexpressing PKM $\zeta$ . Overall, the total fraction of all short (spine length  $< 2 \mu\text{m}$ ) protrusions detected in PKM $\zeta_{OE}$  neurons is significantly higher than in Control neurons. (D) PKM $\zeta$  overexpression leads to an increase in mature spine (stubby + mushroom) density. (E) Overexpression of PKM $\zeta$  does not affect total protrusion density. (F) No significant difference in mature spine density is seen when comparing between 11–12 DIV PKM $\zeta_{OE}$  neurons with 18 DIV neurons of the same transfection group. The same comparison in the Control group shows a significantly higher fraction of mature spines in the 18 DIV neurons. PKM $\zeta_{OE}$ — $n = 10$  cells (total dendritic length: 1956  $\mu\text{m}$ , total number of spines: 1065), Control— $n = 10$  cells (total dendritic length: 2326  $\mu\text{m}$ , total number of spines: 1470), \* $P < 0.05$ , \*\* $P < 0.01$ , \*\*\* $P < 0.001$ , student's  $t$ -test, results were calculated by average per neuron and demonstrate mean  $\pm$  standard error of the mean. Scale bars: 2  $\mu\text{m}$ .

PKM $\zeta_{OE}$  and the Control groups (Kolmogorov-Smirnov normality test,  $d = 0.24$ ,  $P < 0.05$ ,  $n = 36$  and  $d = 0.27$ ,  $P < 0.05$ ,  $n = 27$ , respectively). A nonparametric statistical test yielded a significant difference between the amplitudes of mEPSCs in PKM $\zeta_{OE}$  and Control groups (Mann-Whitney  $U$  Test,  $U = 336$ ,  $P < 0.05$ , Fig. 7C). Furthermore, distribution analysis of all separate mEPSC amplitudes in each group (PKM $\zeta_{OE}$ — $n = 1362$  and Control— $n = 998$ ) yielded a significant difference as well (Mann-Whitney  $U$  Test,  $U = 631652.5$ ,  $P < 0.05$ ). In an attempt to pinpoint the differences in mEPSC amplitudes of neurons overexpressing PKM $\zeta$  compared with control neurons, we reanalyzed the data using the 8 largest mEPSCs of each cell from the 2 min recording period, (comprising a population of 288 mEPSCs in PKM $\zeta_{OE}$  group and 216 events in the control group). Results showed a higher mEPSC amplitude average in the PKM $\zeta_{OE}$  group (Fig. 7D,  $P < 0.01$ , student's  $t$ -test), indicating that the size distribution of these mEPSC subsets was more skewed to the right in the PKM $\zeta_{OE}$  group compared with the Control. Thus, using 2 different approaches to the data analysis, we find significant differences between mEPSC amplitudes in PKM $\zeta$  overexpressing and control neurons.

## Discussion

We found that neurons overexpressing PKM $\zeta$  exhibit shorter spines, primarily of the stubby type, yet did not differ from control neurons in spine density, dendritic arborization, and overall viability. Overexpression was also associated with an increase in the size but not the frequency of mEPSCs. Previous studies have reported enhancement of EPSPs following post-synaptic perfusion of the PKM $\zeta$  protein into CA1 pyramidal cells in hippocampal slices (Ling et al. 2002, 2006; Serrano et al. 2005). However, perfusion of an exogenous protein may circumvent the cellular regulatory mechanisms that control the translation, locale, and function of endogenous PKM $\zeta$ , whereas the insertion of an active plasmid construct is likely to harness the overexpressed protein, or at least part of it, to native cellular control. Nevertheless, despite the divergent experimental systems, it seems there is a conservation of the action of PKM $\zeta$ ; to enhance postsynaptic reactivity to afferent stimulation.

The length of a spine's neck has been suggested to play an important role in the regulation of synaptic input (Araya et al.

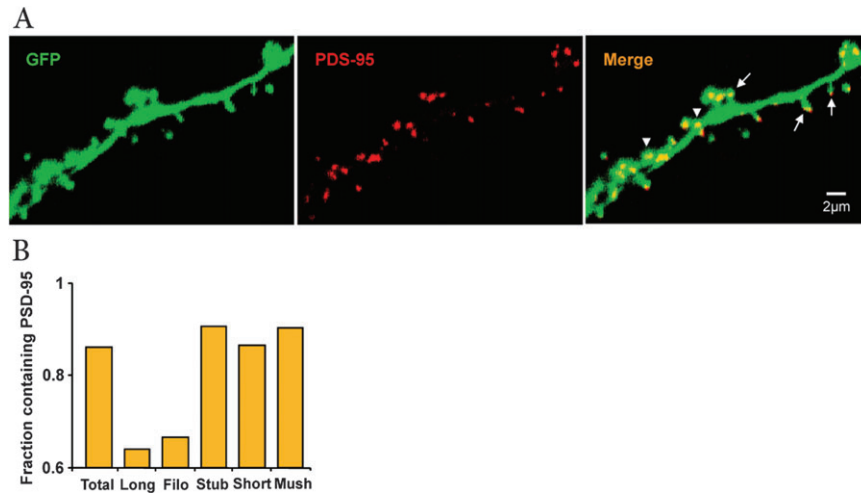


**Figure 6.** Cotransfection of  $PKM\zeta_{OE}$  with PSD-95 confirmed synaptic spines. (A) A representative image of a dendritic segment from a neuron cotransfected with  $PKM\zeta_{OE}$  (represented by the reporter GFP) and PSD-95 (in red). The image shows synapses in the form of stubby spines (arrow heads) as well as synapses of the other forms (arrows). (B) Image analysis identified PSD-95 in more than 85% of all spines and in more than 90% of all stubby spines.  $n = 3$  cotransfected neurons, 336 spines. Thus, more than 85% of the dendritic spines in  $PKM\zeta$  overexpressing neurons, including stubby spines, represent genuine synapses.

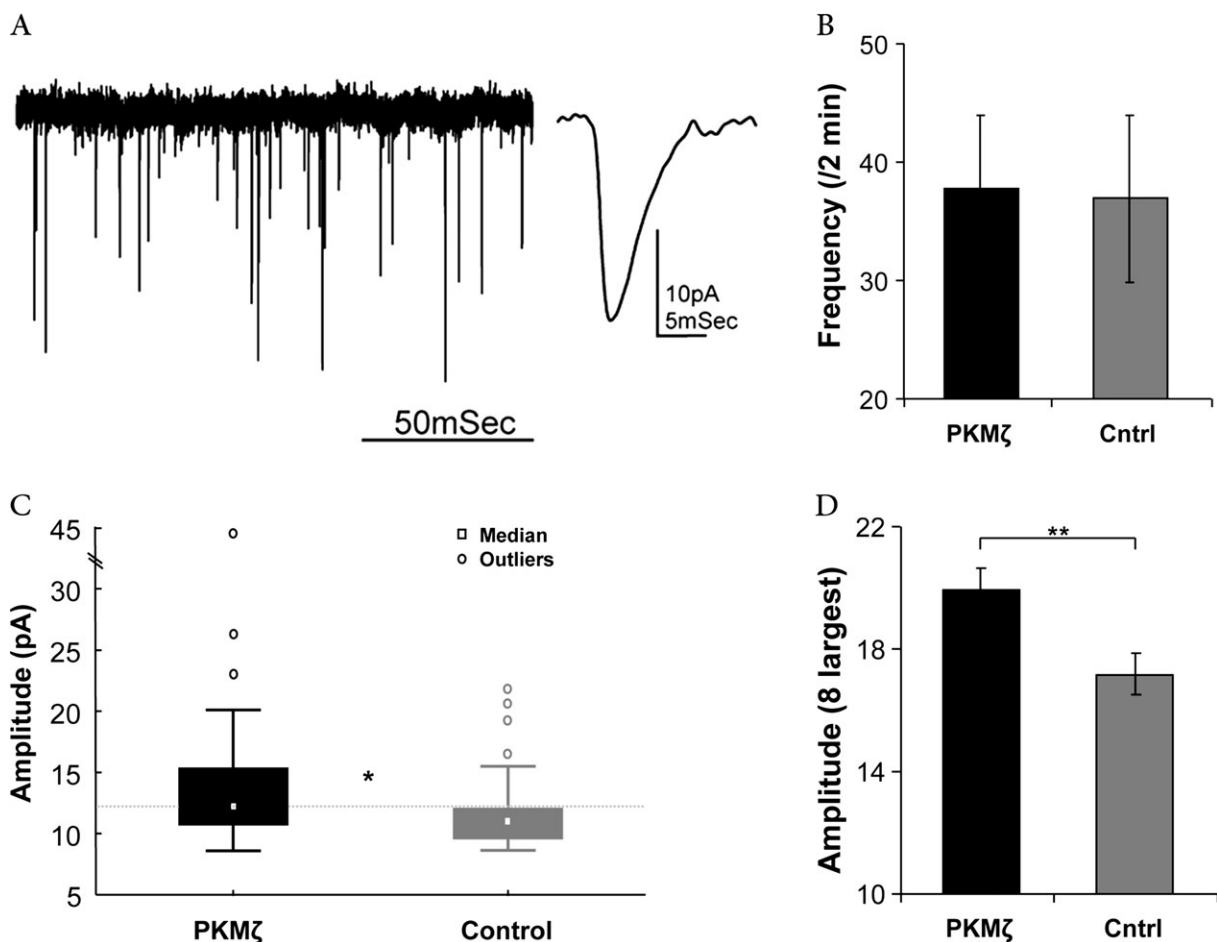


**Figure 7.**  $PKM\zeta_{OE}$  transfected neurons express larger mEPSC amplitudes than controls. (A) Illustration of mEPSCs recorded from a  $PKM\zeta_{OE}$ -transfected neuron, with an expanded trace shown on the right. (B) Frequencies of mEPSCs recorded over a period of 2 min are not different between  $PKM\zeta_{OE}$  ( $n = 36$ ) and Control ( $n = 27$ ) neurons. (C) Box-Whiskers plot of average mEPSC per neuron showing the 25–75 percentile (solid), median, and outliers for each transfection group. Mann-Whitney  $U$  test depicts a significant difference between the amplitudes of mEPSCs in  $PKM\zeta_{OE}$  ( $n = 36$  neurons) and Control ( $n = 27$  neurons) groups. (D) Mean mEPSC amplitude is significantly higher in the  $PKM\zeta_{OE}$  group when collecting the 8 largest mEPSCs from each cell ( $PKM\zeta_{OE}$ — $n = 36$  neurons,  $n = 288$  events and Control— $n = 27$  neurons,  $n = 216$  events).  $*P < 0.05$ —Mann-Whitney  $U$  test.  $**P < 0.01$ —student's  $t$ -test, results are mean  $\pm$  standard error of the mean.

2006; Korkotian and Segal 2007) and of molecular diffusion rates (Ashby et al. 2006) from the spine head to its dendritic base; reduction in the synaptic current is positively correlated with distance from the spine head. This is in line with our finding that PKM $\zeta$  overexpression significantly reduces spine length and increases mEPSC amplitude.

The most significant morphological effect caused by PKM $\zeta$  overexpression was the marked increase in density of stubby spines compared with *Control* and *DN* neurons. Many studies have defined stubby spines as mature formations since they are relatively stable and can persist for months (Irwin et al. 2000; Holtmaat et al. 2005; Restivo et al. 2005; Zuo et al. 2005; Majewska et al. 2006). Thin or long spines tend to represent newly formed synapses and can appear and disappear within days (Holtmaat et al. 2005; Peebles et al. 2010). Furthermore, filopodia are frequently described as short-lived protrusions which may also be precursors of dendritic spines (Ziv and Smith 1996; Portera-Cailliau et al. 2003). Thus, our findings suggest that PKM $\zeta$  overexpression leads to the upregulation of stable more mature spines while downregulating expression of transient less established spines and filopodia. It is noteworthy in this context that maintenance of synaptic efficacy as well as memory storage was posited to indeed require stable memory spines (Holtmaat et al. 2005; Bourne and Harris 2007).

Total spine density was not affected by PKM $\zeta$  overexpression. This result and the aforementioned morphological effects are in line with the hypothesis that newly synthesized PKM $\zeta$  locates preferentially to specific preexisting synapses through a potential “synaptic tagging” mechanism (Sossin 1996; Frey and Morris 1997; Sajikumar et al. 2005; Shema et al. 2011). This model further suggests that “plasticity related proteins” (PRPs), synthesized in dendrites or cell-wide, are directed to specific, recently activated, tagged synapses. It is hence plausible to assume that as a PRP, newly synthesized PKM $\zeta$  accumulates in existing spines and therefore its effect on morphological plasticity leads to structural modification of such spines rather than to spine formation. Therefore, overexpression of PKM $\zeta$  might lead to maturation of a higher number of spines, resulting in the appearance of a smaller fraction of transient ones. PKM $\zeta$  has been linked to neural stabilization in the developing brain of *Xenopus* tadpoles (Liu et al. 2009). These stabilizing effects during dendritogenesis, which suggested premature loss of morphological plasticity in the developing tadpole brain, led these authors to suggest that PKM $\zeta$  may be involved in the morphological maturation of neurons.

Along with stubby spines and even more so, mushroom spines are considered true mature synapses. Our findings show merely a trend toward a higher percentage of such spines in PKM $\zeta$  overexpressing neurons when compared with *DN* and *Control*. It is noteworthy that PKC activation was reported to result in an increase in the number of stubby spines in neurons of hippocampal slices, while PKC activation followed by learning resulted in the transformation of these stubby spines into mushroom spines (Hongpaisan and Alkon 2007). Thus, it is possible that the effect of PKM $\zeta$  on spine maturation in vitro represents an intermediate step of spine maturation in vivo (i.e., from stubby to mushroom or directly to mushroom), which requires specific circuit wiring and synaptic innervations induced by learning stimuli. Further resolution of this possibility might emerge from studies of the effects of PKM $\zeta$  overexpression in vivo (Shema et al. 2011). Interestingly,

although our study examines PSD-95 localization merely for synapse confirmation, PKM $\zeta$  activity has recently been suggested to play an important role in PSD-95 localization (Yoshii et al. 2011). Therefore, future comparison between PSD-95 localization in PKM $\zeta$  overexpressing and control cortical neurons could contribute to the understanding of the role of PKM $\zeta$  in synapse formation.

Another suggested parameter of spine plasticity is spine head size. Spine head enlargement following local spine activation has been reported (Matsuzaki et al. 2004; Zhou et al. 2004; Segal 2005), and it has been suggested that the insertion of glutamate receptors might be the cause for this expansion (Segal 2010). Previous reports imply that PKM $\zeta$  exerts its effects on long-term plasticity through GluR2-AMPA receptor upregulation (Ling et al. 2006; Yao et al. 2008; Migues et al. 2010). Our findings indicate only a trend toward an enlargement of stubby spine heads in PKM $\zeta_{OE}$  neurons compared with *Control* and *DN* neurons.

Our morphometric assessment unveiled no significant differences between neurons expressing the dominant negative form of PKM $\zeta$  and control neurons. This may suggest that the role of PKM $\zeta$  becomes critical only in triggering or maintaining synaptic maturation above a basal functional level, therefore suppressing the constitutive level of the enzyme has no apparent effect on the spine set.

All in all, the results indicate that PKM $\zeta$  can control spine maturation in vitro. This might underlie its reported critical role in maintaining long-term and remote memory in vivo.

### Supplementary Material

Supplementary material can be found at: <http://www.cercor.oxfordjournals.org/>

### Funding

Israel Science Foundation (M.S.) and the Pratt Foundation and the US-Israel Binational Science Foundation Grant 2007141 (Y.D.).

### Notes

We thank Todd C. Sacktor for the PKM $\zeta$  antibody and for the original PKM $\zeta$  sequence. We are grateful to Alon Chen, Sharon Haramati, Shosh Gil, and Reut Shema for supplying the constructs and for valuable discussions. We also thank Efrat Biton, Aya Ben-Yakov, Avi Mendelsohn, Alex Pine, Shoshi Hazvi, Edi Korkotian, Reut Shema, and Eldi Schonfeld for their technical and professional advice. *Conflict of Interest*: None declared.

### References

- Araya R, Jiang J, Eisenthal KB, Yuste R. 2006. The spine neck filters membrane potentials. *Proc Natl Acad Sci U S A*. 103:17961–17966.
- Ashby MC, Maier SR, Nishimune A, Henley JM. 2006. Lateral diffusion drives constitutive exchange of AMPA receptors at dendritic spines and is regulated by spine morphology. *J Neurosci*. 26:7046–7055.
- Bailey CH, Kandel ER. 1993. Structural changes accompanying memory storage. *Annu Rev Physiol*. 55:397–426.
- Bourne J, Harris KM. 2007. Do thin spines learn to be mushroom spines that remember? *Curr Opin Neurobiol*. 17(3):381–386.
- Bourne JN, Harris KM. 2008. Balancing structure and function at hippocampal dendritic spines. *Annu Rev Neurosci*. 31:47–67.
- Camera P, Schubert V, Pellegrino M, Berto G, Vercelli A, Muzzi P, Hirsch E, Altruda F, Dotti CG, Di Cunto F. 2008. The RhoA-associated protein Citron-N controls dendritic spine maintenance by interacting with spine-associated Golgi compartments. *EMBO Rep*. 9(4):384–392.

- De Roo M, Klausner P, Garcia PM, Pogliani L, Muller D. 2008. Spine dynamics and synapse remodeling during LTP and memory processes. *Prog Brain Res*. 169:199-207.
- Frey U, Morris M. 1997. Synaptic tagging and long-term potentiation. *Nature*. 385:533-536.
- Goldin M, Segal M, Avignone E. 2001. Functional plasticity triggers formation and pruning of dendritic spines in cultured hippocampal networks. *J Neurosci*. 21:186-193.
- Hardt O, Miguez PV, Hastings M, Wong J, Nader K. 2010. PKMzeta maintains 1-day- and 6-day-old long-term object location but not object identity memory in dorsal hippocampus. *Hippocampus*. 20(6):691-695.
- Hernandez AI, Blace N, Crary JF, Serrano PA, Leitges M, Libien JM, Weinstein G, Tcherapanov A, Sacktor TC. 2003. Protein kinase M $\zeta$  synthesis from a brain mRNA encoding an independent protein kinase C $\zeta$  catalytic domain. Implications for the molecular mechanism of memory. *J Biol Chem*. 278:40305-40316.
- Holtmaat AJ, Trachtenberg JT, Wilbrecht L, Shepherd GM, Zhang X, Knott GW, Svoboda K. 2005. Transient and persistent dendritic spines in the neocortex in vivo. *Neuron*. 45(2):279-291.
- Hongpaisan J, Alkon DL. 2007. A structural basis for enhancement of long-term associative memory in single dendritic spines regulated by PKC. *Proc Natl Acad Sci U S A*. 104(49):19571-19576.
- Irwin SA, Galvez R, Greenough WT. 2000. Dendritic spine structural anomalies in fragile-X mental retardation syndrome. *Cereb Cortex*. 10(10):1038-1044.
- Kasai H, Hayama T, Ishikawa M, Watanabe S, Yagishita S, Noguchi J. 2010. Learning rules and persistence of dendritic spines. *Eur J Neurosci*. 32:241-249.
- Kelly MT, Crary JF, Sacktor TC. 2007. Regulation of protein kinase Mzeta synthesis by multiple kinases in long-term potentiation. *J Neurosci*. 27(13):3439-3444.
- Kopec CD, Real E, Kessels HW, Malinow R. 2007. GluR1 links structural and functional plasticity at excitatory synapses. *J Neurosci*. 27(50):13706-13718.
- Korkotian E, Segal M. 2007. Morphological constraints on calcium dependent glutamate receptor trafficking into individual dendritic spine. *Cell Calcium*. 42(1):41-57.
- Kwapis JL, Jarome TJ, Lonergan ME, Helmstetter FJ. 2009. Protein kinase Mzeta maintains fear memory in the amygdala but not in the hippocampus. *Behav Neurosci*. 123(4):844-850.
- Lamprecht R, LeDoux J. 2004. Structural plasticity and memory. *Nat Rev Neurosci*. 5:45-54.
- Ling DS, Benardo LS, Sacktor TC. 2006. Protein kinase Mzeta enhances excitatory synaptic transmission by increasing the number of active postsynaptic AMPA receptors. *Hippocampus*. 16(5):443-452.
- Ling DS, Benardo LS, Serrano PA, Blace N, Kelly MT, Crary JF, Sacktor TC. 2002. Protein kinase Mzeta is necessary and sufficient for LTP maintenance. *Nat Neurosci*. 5(4):295-296.
- Liu XF, Tari PK, Haas K. 2009. PKMzeta restricts dendritic arbor growth by filopodial and branch stabilization within the intact and awake developing brain. *J Neurosci*. 29(39):12229-12235.
- Majewska AK, Newton JR, Sur M. 2006. Remodeling of synaptic structure in sensory cortical areas in vivo. *J Neurosci*. 26(11):3021-3029.
- Matsuzaki M, Hinkura N, Ellis-Davies G, Kasai H. 2004. Structural basis of long-term potentiation in single dendritic spines. *Nature*. 429:761-766.
- Miguez PV, Hardt O, Wu DC, Gamache K, Sacktor TC, Wang YT, Nader K. 2010. PKMzeta maintains memories by regulating GluR2-dependent AMPA receptor trafficking. *Nat Neurosci*. 13(5):630-634.
- Osten P, Valsamis L, Harris A, Sacktor TC. 1996. Protein synthesis-dependent potentiation formation of protein kinase Mzeta in long-term potentiation. *J Neurosci*. 16:2444-2451.
- Parrish JZ, Emoto K, Kim MD, Jan YN. 2007. Mechanisms that regulate establishment, maintenance, and remodeling of dendritic fields. *Annu Rev Neurosci*. 30:399-423.
- Pastalkova E, Serrano P, Pinkhasova D, Wallace E, Fenton AA, Sacktor TC. 2006. Storage of spatial information by the maintenance mechanism of LTP. *Science*. 313(5790):1141-1144.
- Peebles CL, Yoo J, Thwin MT, Palop JJ, Noebels JL, Finkbeiner S. 2010. Arc regulates spine morphology and maintains network stability in vivo. *Proc Natl Acad Sci U S A*. 107(42):18173-18178.
- Portera-Cailliau C, Pan DT, Yuste R. 2003. Activity-regulated dynamic behavior of early dendritic protrusions: evidence for different types of dendritic filopodia. *J Neurosci*. 23:7129-7142.
- Restivo L, Ferrari F, Passino E, Sgobio C, Bock J, Oostra BA, Bagni C, Ammassari-Teule M. 2005. Enriched environment promotes behavioral and morphological recovery in a mouse model for the fragile X syndrome. *Proc Natl Acad Sci U S A*. 102(32):11557-11562.
- Sacktor TC. 2011. How does PKM $\zeta$  maintain long-term memory? *Nat Rev Neurosci*. 12:9-15.
- Sacktor TC, Osten P, Valsamis H, Jiang X, Naik MU, Sublette E. 1993. Persistent activation of the zeta isoform of protein kinase C in the maintenance of long-term potentiation. *Proc Natl Acad Sci U S A*. 90:8342-8346.
- Sajikumar S, Navakkode S, Sacktor TC, Frey JU. 2005. Synaptic tagging and cross-tagging: the role of protein kinase Mzeta in maintaining long-term potentiation but not long-term depression. *J Neurosci*. 25(24):5750-5756.
- Segal M. 2005. Dendritic spines and long-term plasticity. *Nat Rev Neurosci*. 6:277-284.
- Segal M. 2010. Dendritic spines, synaptic plasticity and neuronal survival: activity shapes dendritic spines to enhance neuronal viability. *Eur J Neurosci*. 31(12):2178-2184.
- Serrano P, Friedman EL, Kenney J, Taubenfeld SM, Zimmerman JM, Hanna J, Alberini C, Kelley AE, Maren S, Rudy JW et al. 2008. PKMzeta maintains spatial, instrumental, and classically conditioned long-term memories. *PLoS Biol*. 6(12):2698-2706.
- Serrano P, Yao Y, Sacktor TC. 2005. Persistent phosphorylation by protein kinase Mzeta maintains late-phase long-term potentiation. *J Neurosci*. 25(8):1979-1984.
- Shema R, Haramati S, Ron S, Hazvi S, Chen A, Sacktor TC, Dudai Y. 2011. Enhancement of consolidated long-term memory by overexpression of protein kinase Mzeta in the neocortex. *Science*. 331:1207-1210.
- Shema R, Hazvi S, Sacktor TC, Dudai Y. 2009. Boundary conditions for the maintenance of memory by PKMzeta in neocortex. *Learn Mem*. 16(2):122-128.
- Shema R, Sacktor TC, Dudai Y. 2007. Rapid erasure of long-term memory associations in the cortex by an inhibitor of PKMzeta. *Science*. 317:951-953.
- Sholl DA. 1953. Dendritic organization in the neurons of the visual and motor cortices of the cat. *J Anat*. 87(4):387-406.
- Sossin W. 1996. Mechanisms for the generation of synapse specificity in long-term memory: the implications of a requirement for transcription. *Trends Neurosci*. 19(6):215-218.
- von Kraus LM, Sacktor TC, Francis JT. 2010. Erasing sensorimotor memories via PKMzeta inhibition. *PLoS One*. 5(6):e11125.
- Yang G, Pan F, Gan W. 2009. Stably maintained dendritic spines are associated with lifelong memories. *Nature*. 462(7275):920-924.
- Yao Y, Kelly MT, Sajikumar S, Serrano P, Tian D, Bergold PJ, Frey JU, Sacktor TC. 2008. PKM zeta maintains late long-term potentiation by N-ethylmaleimide-sensitive factor/GluR2-dependent trafficking of postsynaptic AMPA receptors. *J Neurosci*. 28(31):7820-7827.
- Yoshii A, Murata Y, Kim J, Zhang C, Shokat KM, Constantine-Paton M. 2011. TrkB and protein kinase Mzeta regulate synaptic localization of PSD-95 in developing cortex. *J Neurosci*. 31(33):11894-11904.
- Yuste R, Bonhoeffer T. 2001. Morphological changes in dendritic spines associated with long-term synaptic plasticity. *Annu Rev Neurosci*. 24:1071-1089.
- Zhou Q, Homma KJ, Poo M. 2004. Shrinkage of dendritic spines associated with long-term depression of hippocampal synapses. *Neuron*. 44(5):749-757.
- Ziv NE, Smith SJ. 1996. Evidence for a role of dendritic filopodia in synaptogenesis and spine formation. *Neuron*. 17(1):91-102.
- Zuo Y, Lin A, Chang P, Gan W. 2005. Development of long-term dendritic spine stability in diverse regions of cerebral cortex. *Neuron*. 46(2):181-189.